Use of Cooperative Unmanned Air and Ground Vehicles for Detection and Disposal of Simulated Mines

Erica Zawodny MacArthur, Donald MacArthur, Carl Crane
University of Florida, Dept. of Mechanical & Aerospace Engineering
Gainesville, Florida 32611

ABSTRACT

The objective of this research is to extend the sensing capabilities of a multi-vehicle ground system by incorporating the environmental perception abilities of unmanned aerial vehicles.

The aerial vehicle used in this research is a Miniature Aircraft Gas Xcell RC helicopter. It is outfitted with a sensor payload containing stereo vision cameras, GPS, and a digital compass. Geo-referenced images are gathered using the above sensors that will be used in this research to create a map of the operating region. The ground vehicle used in this research is an automated Suzuki Mini-Quad ATV. It has the following onboard sensors: single-vision camera, laser range device, digital compass, GPS, and an encoder. The ground vehicle will use the above sensors and the map provided by the helicopter to traverse the region, locate and isolate simulated land mines. The base station consists of a laptop that provides a communication link between the aerial and ground vehicle systems. It also provides the operator with system operation information and statistics.

All communication between the vehicles and the base station is performed using JAUS (Joint Architecture for Unmanned Systems) messages. The JAUS architecture is employed as a means to organize inter-vehicle and intra-vehicle communication and system component hierarchy. The purpose of JAUS is to provide interoperability between various unmanned systems and subsystems for both military and commercial applications. JAUS seeks to achieve this through the development of functionally cohesive building blocks called components whose interface messages are clearly defined. The JAUS architecture allows for a layered control strategy which has specific message sets for each layer of control. Implementation of the JAUS architecture allows for ease of software development for a multi-vehicle system.

This experiment will demonstrate how an air-ground vehicle system can be used to cooperatively locate and dispose of simulated mines.

Keywords: cooperative, helicopter, autonomous, ground vehicle, UAV-UGV collaboration

1. INTRODUCTION

Recently unmanned aerial vehicles (UAVs) have been used more extensively in military operations. The improved perception abilities of UAVs compared with unmanned ground vehicles (UGVs) make them more attractive for surveying and reconnaissance applications. A combined UAV/UGV multiple vehicle system can provide aerial imagery, perception, and target tracking along with ground target manipulation and inspection capabilities. This experiment was conducted to demonstrate the application of a UAV/UGV system for simulated mine disposal operations.

The experiment was conducted by surveying the target area with the UAV and creating a map of the area. The aerial map was transmitted to the base station and post-processed to extract the locations of the targets and develop waypoints for the ground vehicle to navigate. The ground vehicle then proceeded to each of the targets, which simulated the validatation, and disposal of the ordnance. Results include the aerial map, processed images of the extracted ordnances, and the ground vehicle's ability to navigate to the target points.

2. MATHEMATICS

2.1. Camera Model and Geo-Positioning

For this application a precise camera model and an image to global coordinate transformation were developed. This involved finding the intrinsic and extrinsic camera parameters of the camera system attached to the aerial vehicle. The intrinsic camera parameters were determined using a camera calibration toolbox for MATLAB®[1]. A relation between the normalized pixel coordinates and coordinates in the projective coordinate plane was used:

$$\begin{Bmatrix} u_n \\ v_v \end{Bmatrix} = \begin{Bmatrix} \frac{X_c}{Z_c} \\ \frac{Y_c}{Z_c} \end{Bmatrix} \tag{1}$$

The normalized pixel coordinate vector $\tilde{m}$ and the projective plane coordinate vector $\tilde{M}$ are related using (1) and form the projection relationship between points in the image plane and points in the camera reference frame (Fig. 1) where

$$\tilde{m} = \begin{Bmatrix} u_n \\ v_n \\ 1 \end{Bmatrix} \tag{2}$$

$$\tilde{M} = \begin{Bmatrix} X_c \\ Y_c \\ Z_c \\ 1 \end{Bmatrix}. \tag{3}$$

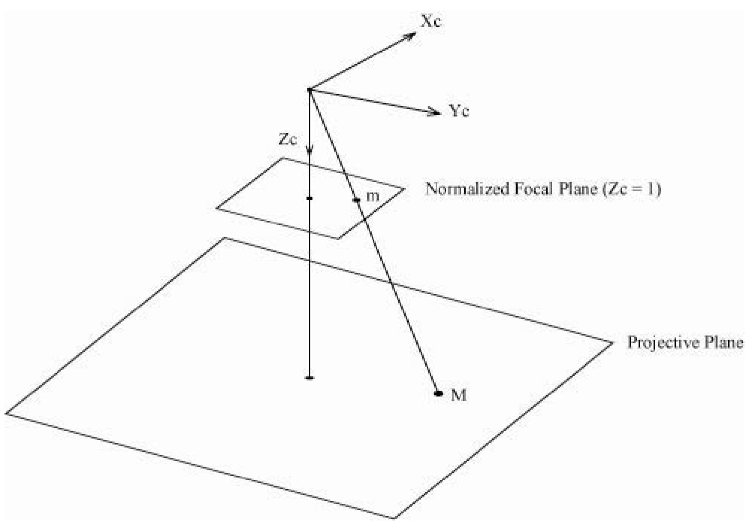

Figure 1: Normalized focal and projective planes

The transformation from image coordinates to global coordinates was determined using the normalized pixel coordinates, and the camera position and orientation with respect to the global coordinate system (Fig.2). The transformation of a point M expressed in the camera reference system C to a point expressed in the global system is shown in (4).

$$^{G}P_{M} = {}^{G}_{C}T\ {}^{C}P_{M} \tag{4}$$

$$^{G}P_{M} = \begin{Bmatrix} X_G \\ Y_G \\ Z_G \\ 1 \end{Bmatrix} = {}^{G}_{C}T\,{}^{C}P_{M} = \begin{bmatrix} {}^{G}_{C}R & {}^{G}P_{Co} \\ 0_3^T & 1 \end{bmatrix} \begin{Bmatrix} X_C \\ Y_C \\ Z_C \\ 1 \end{Bmatrix} \tag{5}$$

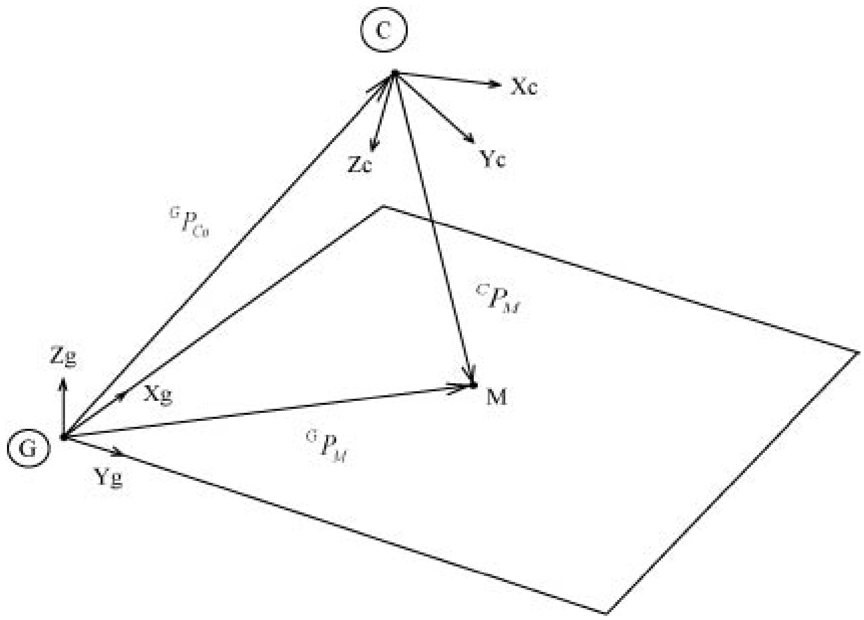

Figure 2: Relation between a point in the camera and global reference frames

Dividing both sides of (5) by Z_C and substituting $Z_W = 0$ (assuming the elevation of the camera is evaluated as the above ground level and the uxo location exists on the $Z_W = 0$ global plane) results in (6).

$$\begin{Bmatrix} \frac{X_G}{Z_C} \\ \frac{Y_G}{Z_C} \\ 0 \\ \frac{1}{Z_C} \end{Bmatrix} = \begin{bmatrix} {}^G_C R & {}^G P_{Co} \\ 0_3^T & 1 \end{bmatrix} \begin{Bmatrix} \frac{X_C}{Z_C} \\ \frac{Y_C}{Z_C} \\ 1 \\ \frac{1}{Z_C} \end{Bmatrix} \tag{6}$$

Substituting $X_C/Z_C = u_n$ an $Y_C/Z_C = v_n$:

$$\begin{Bmatrix} \frac{X_G}{Z_C} \\ \frac{Y_G}{Z_C} \\ 0 \\ \frac{1}{Z_C} \end{Bmatrix} = \begin{bmatrix} {}^G_C R & {}^G P_{Co} \\ 0_3^T & 1 \end{bmatrix} \begin{Bmatrix} u_n \\ v_n \\ 1 \\ \frac{1}{Z_C} \end{Bmatrix} \tag{7}$$

This leads to three equations and three unknowns X_G, Y_G, Z_C:

$$\frac{X_G}{Z_C} = R_{11} u_n + R_{12} v_n + R_{13} + \frac{{}^G P_{Cox}}{Z_C} \tag{8}$$

$$\frac{Y_G}{Z_C} = R_{21} u_n + R_{22} v_n + R_{23} + \frac{{}^G P_{Coy}}{Z_C} \tag{9}$$

$$0 = R_{31} u_n + R_{32} v_n + R_{33} + \frac{{}^G P_{Coz}}{Z_C}. \tag{10}$$

Using (8,9,10) Z_C, X_G, Y_G can be determined explicitly:

$$Z_C = \frac{-{}^G P_{Coz}}{R_{31}u_n + R_{32}v_n + R_{33}} \tag{11}$$

$$X_G = \left(\frac{-{}^G P_{Coz}}{R_{31}u_n + R_{32}v_n + R_{33}}\right)(R_{11}u_n + R_{12}v_n + R_{13}) + {}^G P_{Cox} \tag{12}$$

$$Y_G = \left(\frac{-{}^G P_{Coz}}{R_{31}u_n + R_{32}v_n + R_{33}}\right)(R_{21}u_n + R_{22}v_n + R_{23}) + {}^G P_{Coy} \tag{13}$$

Equations (12, 13) provide the global coordinates of the UXO. These coordinates were then used as waypoints for UGV navigation.

2.2. A* Waypoint Path Planning

Once a set of waypoints was provided by the UAV, the UGV was programmed to visit every waypoint as if to simulate the automated recovery/disposal process of the UXOs. The recovery/disposal process was optimized by ordering the waypoints in a manner that would minimize the total distance traveled by the UGV. This problem was similar to the traveling salesman optimization problem in which a set of cities must all be visited once while minimizing the total distance traveled. An A* search algorithm was implemented in order to solve this problem.

The A* search algorithm operates by creating a decision graph and traversing the graph from node to node until the goal is reached. For the problem of waypoint order optimization, the current path distance *g*, estimated distance to the final waypoint $\hat{h}$, and the estimated total distance $\hat{f}$ was evaluated for each node by

$$g = \sum \text{ length of straight line segments of all predecessor waypoints} \tag{14}$$

$$\hat{h} = \text{(minimum distance of any two waypoints} \in \text{(successors \& current waypoints))} \times \text{(\# of successors)} \tag{15}$$

$$f = g + \hat{h}. \tag{16}$$

The requirement for the A* algorithm of the admissibility of the $\hat{h}$ heuristic is fulfilled due to the fact that there exists no path from the current node *n* to a goal node with a distance less than $\hat{h}$. Therefore the heuristic provides the minimum bound as required by the A* algorithm and guarantees optimality should a path exist.

3. EXPERIMENTAL TESTBED

3.1. Unmanned Ground Vehicle Specifications

The unmanned ground vehicle platform was an automated all terrain vehicle. It was developed using a stock two cycle gasoline powered Suzuki Mini-Quad ATV (Fig. 2). The vehicle's existing steering was equipped with an Animatics servo motor with integrated encoder, controller, and amplifier. Throttle and brake cables were actuated using two RC style servo motors. In addition, the vehicle was equipped with onboard and RF remote kill switches, 1KW gas powered Honda generator, UPS power backup system, and power regulation/conditioning electronics.

The UGV was equipped with two computing nodes. The POS computing node interfaced to the GPS, digital compass, and encoder to provide the position and orientation information to the system. The SSC computing node handled high level communication with the base station as well as vehicle control and automation tasks.

3.1.1. System Architecture

The UGV system consists of a base station (laptop computer), the vehicle, and all of its onboard sensors and computers. Autonomous vehicle navigation is realized using a combination of the following sensors: Garmin GPS 16, PNI digital compass, and an incremental encoder. Filtering of all of these sensors provides the vehicle with repeatable and accurate navigation to two meters. The UGV receives all of its commands from the base station. All communications are via wireless Ethernet.

3.2. Unmanned Aerial Vehicle Specifications

The unmanned aerial vehicle was composed of a Miniature Aircraft Gas Xcell RC helicopter. The helicopter had a six foot rotor diameter and can lift approximately 15 pounds. A custom built sensor/electronics payload was integrated into the airframe of the aircraft and provided image data, position, and orientation information.

3.2.1. System Architecture

The aircraft sensor payload was designed to be completely modular. The system had self contained power, computation, data storage, and communication components. It had custom Lithium Polymer battery packs which provided power to all of the onboard components. The system had a Garmin GPS 16A commercial 5Hz WAAS gps which provided the global position of the aircraft, and a PNI digital compass which provided the heading and attitude of the aircraft. The system was also equipped with a Videre Stereovision System which allowed for high resolution stereo and monocular images to be collected. The system was also equipped with dual flash memory drives which provided robust data storage even in the aircraft's dynamic vibration environment. During testing, the data was collected in sync where the images, GPS position, and orientation were all collected at the same instant and stored for post processing. The system was also equipped with a wireless Ethernet communication which allowed for streaming video and status information to be viewed at the base-station.

Figure 2: TailGator and HeliGator Platforms

4. EXPERIMENTAL SETUP

4.1. Waypoint Surveying

In order to evaluate the performance of the UAV/UGV system, the waypoints were surveyed using a Novatel RT-2 differential GPS. This system provided two centimeter accuracy or better when provided with a base station correction signal. Accurate surveying of the visited waypoints provided a baseline for comparison of the results obtained from the helicopter and the corresponding path the ground vehicle traversed.

The UXOs were simulated to resemble BLU-97 ordnance. Aerial photographs (Fig. 3) of the ordnance along with the camera position and orientation were collected. Using the transformation described previously the global coordinates of the UXOs were calculated. The calculated UXO positions were compared with the precision survey data.

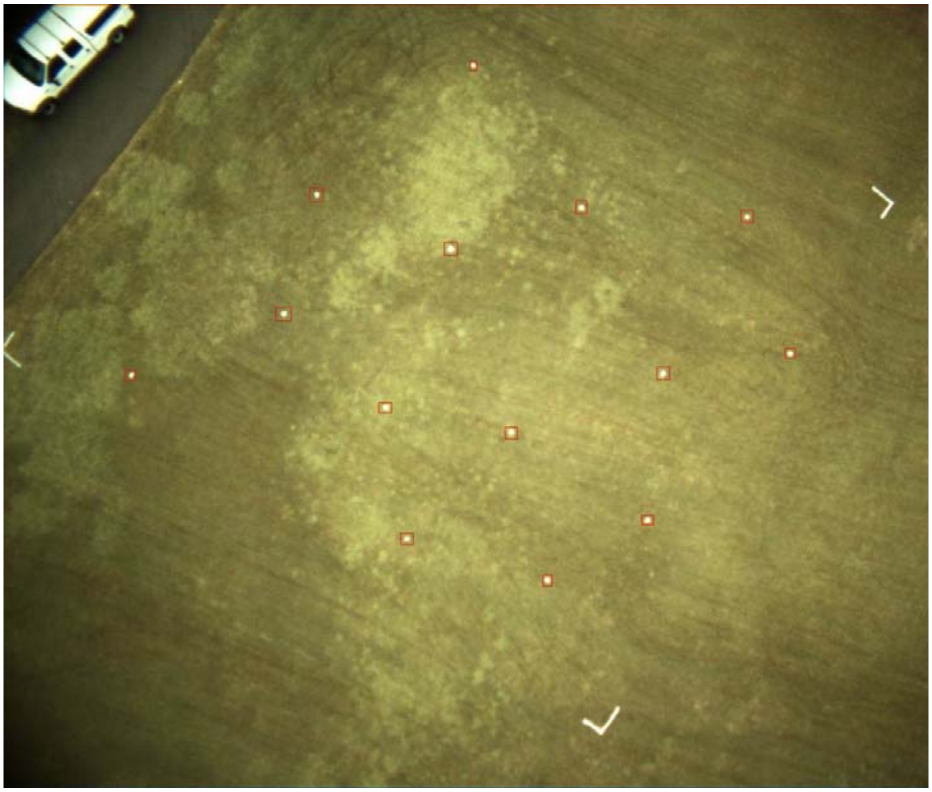

Figure 3: Aerial photograph of all UXOs

4.2. Local Map

A local map of the operating region was generated using the precision survey data. This local map (Fig. 4) provided a baseline for all of the position comparisons throughout this paper.

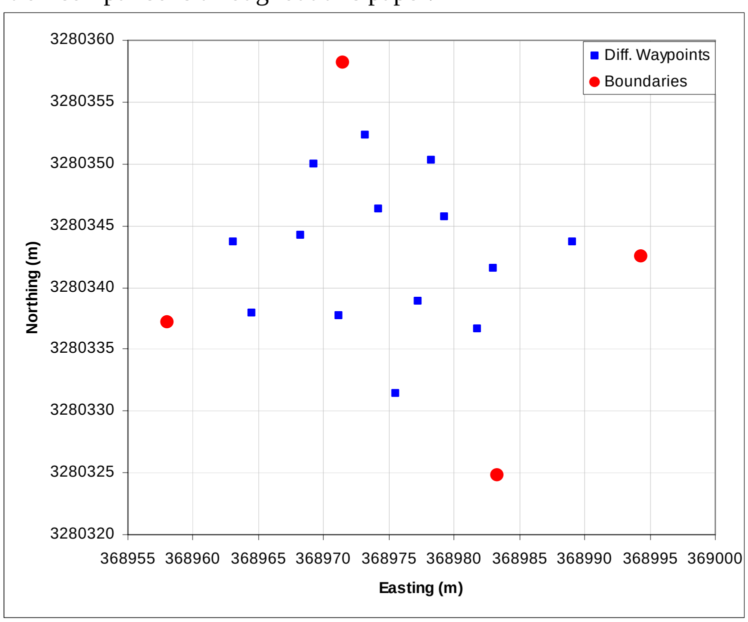

Figure 4: Local map generated with Novatel differential GPS

5. RESULTS

The data collected compares the positioning ability of the UGV and the ability of the UAV sensor system to accurately calculate the UXO positions. While both the UGV and UAV use WAAS enabled GPS there is some inherent error due to vehicle motion and environmental affects. The UGV's control feedback was based on waypoint to waypoint control versus a path following control algorithm. The UGV was commanded to come within a specified threshold of a waypoint before switching to the next waypoint (Fig. 5). The UGV consistently traveled within three meters or less of each of the desired waypoints which is within the error envelope of typical WAAS GPS accuracy.

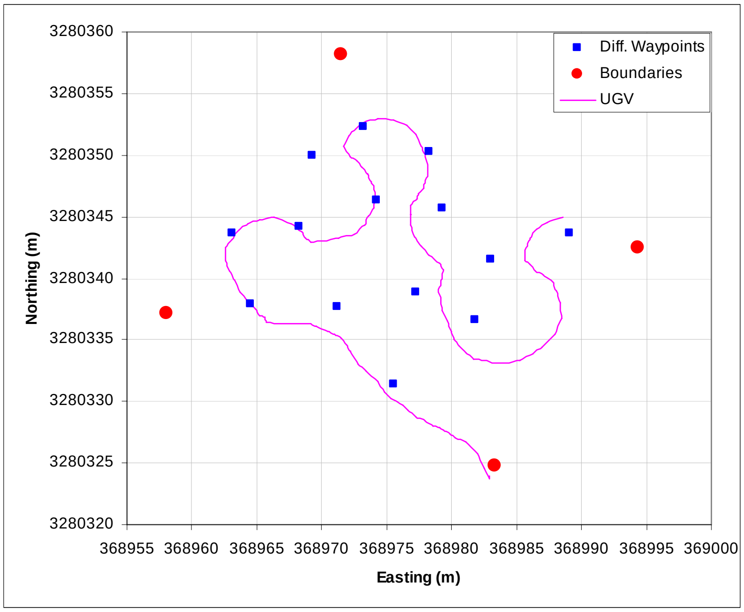

Figure 5: A comparison of the UGV's path to the differential waypoints

The UAV calculates the waypoints based on its sensors and these points are compared with the surveyed waypoints. There is an offset in the UAV's data due to the GPS being used and due to error in the transformation from image coordinates to global coordinates (Fig. 6). In addition, the waypoints that the UAV determined were given directly to the UGV once they were sorted (Fig. 7).

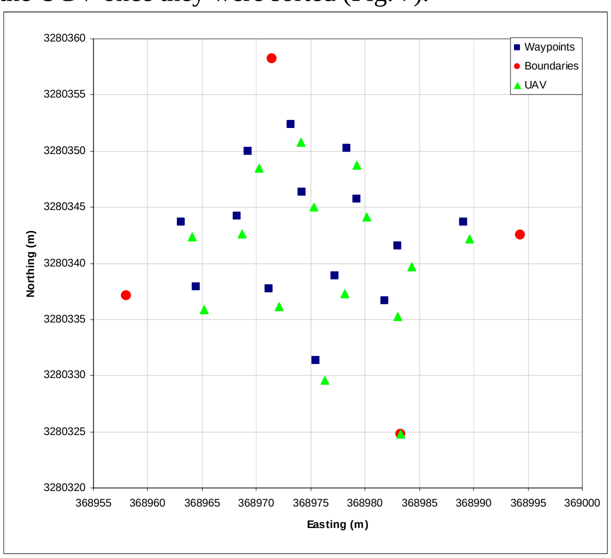

Figure 6: UAV vs. Differential GPS

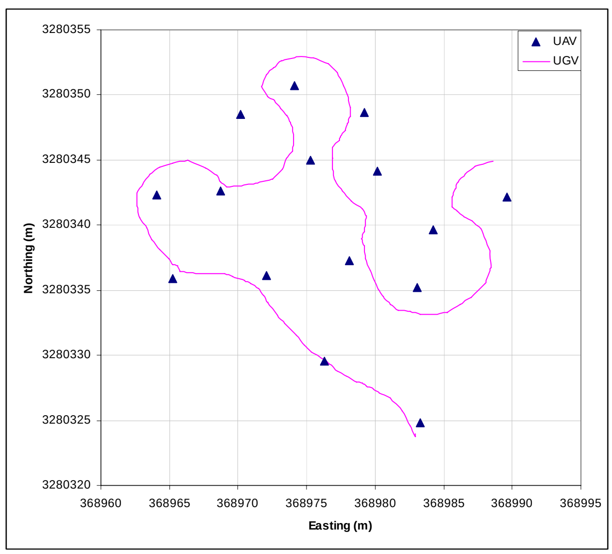

Figure 7: UAV waypoints vs. UGV path

The UGV is able to navigate within several meters of the waypoints, however, is limited due to the vehicle kinematics. Further work involves a waypoint sorting algorithm that accounts for the turning radius of the vehicle.

6. CONCLUSION

This paper has presented the research involving UAV/UGV collaboration for simulated mine disposal. The results obtained demonstrate that the UAV system can be used to determine the UXO positions using aerial imagery. The experiment then showed that a UGV could then navigate to the UXO positions based on the UAV data. This system utilizes the perception abilities of UAV systems and has demonstrated a possible application in a heterogeneous multiple vehicle system.

The results show that the UGV is greatly affected by its inherent kinematic constraints. Due to its Ackermann steering system, the path that the UGV can traverse is limited by the minimum turning radius. The analysis did not include kinematic constraints into the waypoint sorting algorithm. Also the UGV control algorithm was waypoint based versus a continuous path based approach. Future research will incorporate UGV kinematic and dynamic constraints into the vehicle control strategies. In addition, the optimal path search will consist of a series of continuous path segments rather than discreet waypoint. Both of these changes to the current approach hope to improve overall system performance.

ACKNOWLEDGEMENTS

This research was conducted in collaboration with the Tyndall Air Force Base Robotics Research Laboratory in Panama City, Florida.

REFERENCES

1. Bouguet, J., Camera Calibration Toolbox for MATLAB®, http://www.vision.caltech.edu/bouguetj/calib_doc/.
2. Crane, C., Duffy, J., Kinematic Analysis of Robot Manipulators, Cambridge University Press, 1998.
3. Faugeras, O., Luong, Q., The Geometry of Multiple Images, The MIT Press, 2001.
4. Nilsson, N., Artificial Intelligence: A New Synthesis, San Francisco: Morgan Kaufmann, 1998.